Hydrogenation inducing antiferromagnetism in the heavy-fermion ternary silicide CeRuSi

B. Chevalier,[1,*] E. Gaudin,[1] S. Tencé,[1,4] B. Malaman,[2] J. Rodriguez Fernandez,[3] G. André,[4] and B. Coqblin[5]
[1]*Institut de Chimie de la Matière Condensée de Bordeaux (ICMCB), CNRS, Université Bordeaux 1, 87 Avenue du Docteur Albert Schweitzer, 33608 Pessac, France*
[2]*Laboratoire de Chimie du Solide Minéral, Associé au CNRS [UMR 7555], Université Henri Poincaré-Nancy1, Boîte Postale 239, 54506 Vandoeuvre les Nancy Cedex, France*
[3]*CITIMAC, Facultad de Ciencias, Universidad de Cantabria, 39005 Santander, Spain*
[4]*Laboratoire Léon Brillouin (LLB), CEA/CNRS, 91191 Gif-Sur-Yvette Cedex, France*
[5]*Laboratoire de Physique des Solides, Université Paris-Sud, CNRS, UMR 8502, 91405 Orsay, France*
(Received 3 July 2007; revised manuscript received 26 October 2007; published 11 January 2008)

The hydride $CeRuSiH_{1.0}$ with space group $P4/nmm$ was synthesized by exposure at 523 K of the heavy-fermion ternary silicide CeRuSi under 4 MPa of hydrogen gas. The investigation of the hydride by x-ray powder diffraction reveals that the hydrogenation induces a pronounced anisotropic expansion of the unit cell. Moreover, $CeRuSiH_{1.0}$ presents two antiferromagnetic transitions at $T_{N1}=7.5(2)$ K and $T_{N2}=3.1(2)$ K evidenced by magnetization and specific heat measurements. Hydrogenation changes the moderate heavy-fermion compound CeRuSi, which has a $\gamma=220$ mJ/mol K^2, to an antiferromagnet, which has a smaller electronic coefficient $\gamma=26$ mJ/mol K^2. In other words, the hydrogen insertion diminishes the influence of the Kondo effect. The transition heavy-fermion behavior→antiferromagnet can be well understood in terms of the classical Doniach diagram where the hydrogenation plays a role opposite to the pressure. The expansion of the lattice induced by hydrogen insertion is here much more important than the role of Ce-H bonding observed in other hydrogenated compounds $CeCoSiH_{1.0}$ or $CeCoGeH_{1.0}$, where an opposite transition (antiferromagnetic →spin fluctuation) was evidenced.

DOI: 10.1103/PhysRevB.77.014414 PACS number(s): 75.50.Lk, 61.66.Dk, 65.40.Ba, 71.27.+a

I. INTRODUCTION

During the past decades, many intermetallics have been involved in the enormous research effort devoted to the hydrogenation-induced changes of their magnetic properties.[1] The hydrogen insertion in compounds absorbing it, is an interesting way to modify the magnetic interactions, which are very sensitive to the change of the interatomic distances.[2] Generally, the hydrogen absorption leads to an increase of the unit cell volume and can be considered as a negative pressure. However, in addition to this steric effect, the presence of $1s$(H) electrons causes a modification of the electronic structure with the creation of an additional low s band and a change of the density of states at the Fermi level. To illustrate the influence of hydrogenation on the magnetic properties of intermetallics, we can quote as examples an increase in the Curie temperature of (i) Nd_2Fe_{17} from 330 to 448 K by hydrogen insertion (this effect is connected to the increase in average Fe-Fe distances[3,4]) and (ii) UCoSn from 82 to 102 K after hydrogen absorption (the lattice expansion induces a reduction of the $5f$-$5f$ overlap and then an increase of the localization of the $5f$(U) states.[5]

The role of hydrogenation has been recently studied in many cerium ternary compounds, such as CeCoSi, CeCoGe, CeFeSi, CeMnGe,[6–10] and CeNiGa,[11] but different effects on their physical properties have been observed.

Hydrogen insertion in CeCoSi and CeCoGe, crystallizing in the tetragonal CeFeSi-type structure, leads to the destruction of their antiferromagnetic properties. For instance, CeCoSi shows a Néel temperature of 8.8(2) K, whereas $CeCoSiH_{1.0}$ presents a spin fluctuation behavior below $T_{sf}=130(5)$ K.[2,4,5] In order to explain this antiferromagnetism to spin fluctuation transition, the electronic and magnetic structures of CeCoSi and its hydride were self-consistently calculated within the local spin-density-functional theory[7] and the demagnetization of cerium at low temperatures in $CeCoSiH_{1.0}$ could be associated with the strong Ce-H interaction, which is bonding throughout the conduction band. The hydrogenation of the ternary germanide CeCoGe also undergoes a similar transition from antiferromagnetism with $T_N=5.0$ K to a spin fluctuation behavior below $T_{sf}=15$ K.[9,10] In the two hydrides $CeCoSiH_{1.0}$ and $CeCoGeH_{1.0}$, it appears that the presence of strong Ce-H bonding, which leads to a demagnetization of cerium, prevails over the cell expansion effect, which tends to stabilize the trivalent cerium.

This agrees with the recent investigation of the hydrides $CeCoSiH_{1.0}$, $CeCoGeH_{1.0}$, and $LaCoGeH_{1.0}$ by ^{1}H nuclear magnetic resonance (NMR).[10] For $LaCoGeH_{1.0}$, the position of the isotropic ^{1}H magic angle spinning NMR signal is 8.7 ppm (chemical shift referred to tetramethylsilane), showing no significant Knight shift contribution. On the contrary, the signal for the hydrides based on cerium is strongly shifted to about 150 ppm, which suggests a Fermi contact interaction (transfer of some density of electron spin from Ce to proton via orbital overlap). In other words, the hydrogenation of the ternary compounds adopting the tetragonal CeFeSi-type structure allows us to study the influence on their physical properties of the competition between the increase of the unit cell volume linked to the H insertion and the occurrence of the Ce-H chemical bonding. We note that an increase of the Ce-H interatomic distance (2.391 Å →2.410 Å) (Refs. 6 and 7) in the sequence $CeCoSiH_{1.0}$ →$CeCoGeH_{1.0}$ induces a decrease of the spin fluctuation temperature from 130(5) to 15 K.[7,9]

A different behavior is reported, for instance, after the hydrogenation of the ternary gallide CeNiGa.[11] This compound is characterized by an intermediate valence behavior, while a clear Kondo behavior is observed in the hydride $CeNiGaH_{1.1}$. In particular, this hydride presents a very characteristic log T dependence of the electrical resistivity (ρ) at both low and high temperatures. Moreover, the curve $\rho = f(T)$ exhibits a maximum at roughly 100 K corresponding to a crystal field splitting.[12] Thus, the effect of hydrogen changes the intermediate valence behavior to a weak Kondo one and is, therefore, opposite to the effect of an applied pressure.

Thus, the extensive study of hydrogenated cerium compounds has shown the complex role of hydrogen absorption in these compounds. In the present paper, we will discuss the effect of hydrogenation on the ternary silicide CeRuSi, which crystallizes in the tetragonal CeFeSi-type structure and is considered as a nonmagnetic heavy-fermion system.[13] Its investigation by specific heat (C_p) measurements reveals a shallow maximum at 0.5 K and an electronic coefficient $\gamma = C_p/T = 220$ mJ/mol K^2, which is indicative of a moderate heavy-fermion character. This low-temperature behavior can be associated with the formation of a coherent heavy-fermion ground state, and the analysis of the specific heat measurements within the one-impurity Kondo model has suggested a large Kondo temperature of the order of 25 K.[13] The absence of magnetic ordering for CeRuSi was confirmed above 4.2 K by neutron powder diffraction.[14] Finally, x-ray absorption spectroscopy at the Ce L_{III} edge gives a measured valence of 3.14 for cerium in this ternary silicide.[15] Thus, CeRuSi appears to be a nonmagnetic, almost trivalent and moderate heavy-fermion compound.

The crystal structure of CeRuSi can be described by a stacking along the c axis of two layers formed by $[Ce_4Ru_4]$ antiprisms and separated by one layer of $[Ce_4]$ pseudotetrahedral units.[14] The $[Ce_4Ru_4]$ antiprisms surrounding the Si atom are also observed in the crystal structure of the ternary silicide $CeRu_2Si_2$ considered also as a moderate heavy-fermion compound ($\gamma = 385$ mJ/mol K^2) (Refs. 16–18) showing no evidence of long-range magnetic ordering down to ~20 mK.[19] In addition, the $[Ce_4]$ pseudotetrahedral units are interesting as possible H sites. The compound CeRuSi is isomorphous to the previously studied ternary compounds CeCoSi, CeCoGe, CeFeSi, and CeMnGe.[6–10] The resulting hydrides crystallize as the parent compounds in the tetragonal CeFeSi-type structure where H atoms are inserted in the $[Ce_4]$ tetrahedral interstices. This hydrogenation induces an increase of the unit cell volume (for instance, 7.8% in the sequence $CeCoSi \rightarrow CeCoSiH_{1.0}$)[7] and also a pronounced anisotropic expansion of the unit cell: the a parameter decreases, whereas the c parameter increases.[6–8]

In this view, it is interesting to investigate the hydrogenation of the ternary silicide CeRuSi having a unit cell volume higher than that of CeCoSi or CeCoGe. We report here on the investigation of the new hydride $CeRuSiH_{1.0}$ by x-ray diffraction on single crystal, magnetization, electrical resistivity, thermoelectric power, and specific heat measurements. We will show that this hydride is an antiferromagnet presenting a complex magnetic phase diagram. We discuss these physical properties in relation to those previously reported on the heavy-fermion $CeRu_2Si_2$ where a long-range order can be induced by the replacement of Ce by La (Refs. 17 and 20) or Si by Ge (Ref. 18) (corresponding to a negative pressure effect). Also, for comparison, some results concerning the influence of the hydrogenation of the isomorphous ternary silicide LaRuSi are presented.

II. EXPERIMENTAL DETAILS

A polycrystalline CeRuSi sample was synthesized by arc-melting a stoichiometric mixture of pure elements (purity above 99.9%) in a high-purity argon atmosphere. Then, the sample was turned and remelted several times to ensure homogeneity; the maximum weight loss due to the melting process was equal to 0.2%. Annealing was done for one month at 1073 K by enclosing the sample in an evacuated quartz tube. X-ray powder diffraction detects no parasitic phase and confirms that this ternary silicide crystallizes in the tetragonal CeFeSi-type structure with the unit cell parameters $a = 4.198(2)$ Å and $c = 6.892(2)$ Å, which agree with those reported previously.[14] A similar procedure was used in order to obtain a LaRuSi compound [$a = 4.231(1)$ Å and $c = 7.109(1)$ Å].

Hydrogen absorption experiments were performed using the apparatus described previously.[21] An annealed ingot of CeRuSi (or LaRuSi) was heated under vacuum at 523 K for 12 h and then exposed for 2 days under 4 MPa of hydrogen gas at the same temperature. The duration time for hydrogenation was determined using the first hydrogen absorption, as reported previously.[6] The amount of H inserted was determined volumetrically by monitoring pressure changes in a calibrated volume. Under the experimental conditions described above, CeRuSi (or LaRuSi) absorbs hydrogen. The amount of H atom inserted is 1.0(1) per CeRuSi (or LaRuSi) f.u. The hydride formed is stable in air and shows a metallic aspect. Also, the H absorption induces a decrepitation in small grains of the pure starting ingot.

X-ray powder diffraction with the use of a Philips 1050 diffractometer (Cu $K\alpha$ radiation) was applied for the characterization of the structural type and for the phase identification of the hydride sample. The unit cell parameters were determined by a least-squares refinement method using silicon (5N) as an internal standard. The refinement of the crystal structure of $CeRuSiH_{1.0}$ was performed using a tiny single crystal isolated from the pulverized sample and selected by optical microscopy. Reflection data were collected at room temperature on an Enraf-Nonius Kappa charge coupled device (CCD) area-detector diffractometer using Mo $K\alpha$ radiation. A Gaussian-type absorption correction was applied, the shape of the crystal being determined with the video microscope of the diffractometer. Data processing and all refinements were performed with the JANA2000 program package.[22] Details of data collections and structure refinements are listed in Table I.

For transport measurements, the hydrides $CeRuSiH_{1.0}$ and $LaRuSiH_{1.0}$ were compacted at room temperature (compactness $\cong 80\%$) in order to form a polycrystalline pellet (diameter=6 mm and thickness=3 mm) and then heated

TABLE I. Crystallographic data and structure refinement for $CeRuSiH_{1.0}$.

Crystal data	
Chemical formula	$CeRuSiH_{1.0}$
Molar mass (g mol^{-1})	270.28
Temperature	293 K
Crystal system	Tetragonal
Space group	$P4/nmm$ (No. 129)
Unit cell dimension (Å)	$a=4.1798(5)$[a]
	$c=7.5120(7)$[a]
Volume (Å^3)	131.24(4)[a]
Z (f.u. per unit cell)	2
Calculated density (g cm^{-3})	6.842(6)
Radiation and wavelength (Å)	Mo K_α: 0.71073
Absorption coefficient (mm^{-1})	23.04
$F(000)$	232
Crystal color	Metallic luster
Crystal size (mm)	$0.02\times0.03\times0.06$
Data collection	
Diffractometer	Enraf-Nonius Kappa CCD area detector
θ range for data collection	5°–35°
hkl range	$-5\leqslant h\leqslant 6, -5\leqslant k\leqslant 6, -10\leqslant l\leqslant 11$
Measured reflections	1929
Absorption correction	Gaussian method
Independent reflections	176 ($R_{int}=0.0901$)
Refinement	
Refinement on	F^2
No. of independent reflections	176
No. of observed reflections [$I>3\sigma(I)$]	144
No. of parameters	9
$R(F)$	0.0296
$wR(F)$	0.0686
S	1.41
Difference Fourier residues (e Å^{-3})	+2.03 and −1.57

[a]Deduced from x-ray powder diffraction.

for 2 days at 523 K under pressure (4 MPa) of hydrogen. After this thermal treatment, which improves the mechanical behavior, the pellet was checked by x-ray diffraction; no structural change was evidenced. Thermoelectric power measurements were performed on this pellet using a dynamic method. Details of the cell used and measurement methods were described previously.[23] For electrical resistivity, a bar of $1.5\times1.5\times5$ mm^3 was cut from the pellet. The measurement was carried out above 4.2 K using the standard dc four probe method with silver paint contacts and an intensity current of 10 mA. Finally, magnetization measurements were performed on a part of the pellet using a superconducting quantum interference device magnetometer in the temperature range of 1.8–300 K and applied fields up to 4.6 T. Similar measurements were performed on the initial ternary silicides CeRuSi and LaRuSi obtained after annealing. In order to compare the electrical resistivity of CeRuSi, its hydride, and its homologous compound based on lanthanum, we have used similar bars (same size) and similar contact positions. These conditions minimize the difference between the geometrical factors.

Heat capacity measurements on hydride $CeRuSiH_{1.0}$ were performed by a relaxation method with a Quantum Design PPMS system and using a two tau model analysis. Data were taken in the 1.8–50 K temperature range. For these latter measurements, the sample was a plate of 48.6 mg weight obtained from the same pellet used for the transport and magnetization measurements.

III. RESULTS AND DISCUSSION

A. Crystallographic properties

The structure of $CeRuSiH_{1.0}$ has been determined from single-crystal x-ray data. The extinction conditions observed agree with the $P4/nmm$ space group (No. 129) already used for the refinement of the initial ternary silicide CeRuSi.[14] The starting atomic positions were those reported previously for this last compound [Ce in the $2c$ site (1/4 1/4 0.676), Ru in the $2a$ site (3/4 1/4 0), and Si in the $2c$ site (1/4 1/4 0.173)]. With anisotropic displacement parameters, the final residual factors converged to the values $R(F)=0.0296$ and $wR(F)=0.0686$ for nine refined parameters and 144 observed reflections (Table I). The final atomic positions and anisotropic displacement parameters are given respectively in Tables II and III.

The crystal structure of CeRuSi and its hydride adopt the same space group, but the hydrogenation of this ternary silicide causes a pronounced anisotropic expansion of the unit cell; the a parameter decreases weakly from 4.197(1) to 4.1798(5) Å (−0.41%), whereas the c parameter increases strongly from 6.894(4) to 7.5120(7) Å (+8.96%). In other words, the insertion of hydrogen into CeRuSi involves an expansion of the unit cell volume from 121.4 to 131.24 Å^3 (+8.1%). The strong increase of the c/a ratio ($1.64\rightarrow1.80$) observed after hydrogenation could play

TABLE II. Positional and equivalent isotropic displacement parameters U_{eq} (Å^2) for $CeRuSiH_{1.0}$.

Atom	Site	x	y	z	U_{eq}
Ce	$2c$	1/4	1/4	0.66935(10)	0.0077(2)
Ru	$2a$	3/4	1/4	0	0.0055(2)
Si	$2c$	1/4	1/4	0.1498(5)	0.0077(7)

TABLE III. Anisotropic displacement parameters U^{ij} (Å^2) for $CeRuSiH_{1.0}$.

Atom	U^{11}	U^{22}	U^{33}	U^{12}	U^{13}	U^{23}
Ce	0.0065(3)	0.0065	0.0101(4)	0	0	0
Ru	0.0035(3)	0.0035	0.0096(5)	0	0	0
Si	0.0056(10)	0.0056	0.0119(15)	0	0	0

an important role on the modification of the crystal electric field effect in the sequence $CeRuSi \rightarrow CeRuSiH_{1.0}$ (see below the physical properties). It is also worth pointing out that the H insertion into CeRuSi also affects strongly the atomic position of the Si atom: z_{Si} varies from 0.173(3) (Ref. 14) to 0.1498(5) (Table II); the Si atom shifts along the *c* axis in the $[Ce_4Ru_4]$ antiprisms. On the contrary, z_{Ce} is less affected $[0.676(2) \rightarrow 0.66935(10)]$ by the H insertion.

The strong increase of the *c* parameter in the sequence $CeRuSi \rightarrow CeRuSiH_{1.0}$ suggests that the H atoms are inserted in the $[Ce_4]$ pseudotetrahedral sites, as observed previously for the deuteride $CeCoGeD_{1.0}$.[8] This insertion explains the strong displacement (z_{Si}) of the Si atom along the *c* axis; indeed, the Si-H bonding exists only in this direction. According to this hypothesis, the H atom occupies the 2*b* site (1/4 3/4 1/2), giving interatomic distances $d_{Ce\text{-}H}=2.447$ Å between Ce and H atoms higher than that reported for the hydrides $CeCoSiH_{1.0}$ ($d_{Ce\text{-}H}=2.391$ Å) (Ref. 7) and $CeCoGeH_{1.0}$ ($d_{Ce\text{-}H}=2.410$ Å).[6] This result indicates that the chemical bonding between Ce and H in $CeRuSiH_{1.0}$ is smaller than that existing in other isomorphous hydrides based on cobalt. Neutron powder diffraction experiments need to be performed on $CeRuSiD_{1.0}$ deuteride in order to verify this crystallographic hypothesis.

Table IV compares the interatomic distances between the Ce atom and its ligands for CeRuSi, its hydride, and $CeRu_2Si_2$. In $CeRuSiH_{1.0}$, the distances $d_{Ce\text{-}Ru}=3.246$ Å and $d_{Ce\text{-}Si}=3.253$ Å existing in the $[Ce_4Ru_4]$ antiprisms surrounding the Si atom are comparable to those observed in the ternary silicide $CeRu_2Si_2$, 3.225 and 3.249 Å, respectively.[24] The hydrogenation of CeRuSi induces an increase of these distances. In other words, many structural characteristics of the $[Ce_4Ru_4]$ antiprisms found in $CeRuSiH_{1.0}$ are in agreement with those observed in $CeRu_2Si_2$. This ternary silicide is considered as a moderate heavy fermion showing short-range magnetic correlations at low temperatures.[25] This last behavior is a general feature of heavy-fermion compounds, which are located close to the nonmagnetic $\rightarrow$ magnetic transition.

A similar change of the unit cell parameters is observed during the hydrogenation of LaRuSi. In this case also, the *a* parameter decreases from 4.231(1) to 4.202(1) Å (−0.69%), whereas the *c* parameter increases from 7.109(1) to 7.721(1) Å (+8.61%).

B. Magnetization

Figure 1 compares the temperature dependence of the reciprocal magnetic susceptibility χ_m^{-1} of CeRuSi and its hydride. In the whole temperature range of 1.8–300 K, the data for CeRuSi can be fitted with a Curie-Weiss law, $\chi_m^{-1}=(T-\theta_p)/(0.125\mu_{eff}^2)$, giving $\theta_p=-81$ K as a paramagnetic Curie temperature and $\mu_{eff}=2.60(2)\mu_B$/Ce mol as a magnetic effective moment. These values are slightly different from those reported previously ($\mu_{eff}=2.56\mu_B$/Ce mol and $\theta_p=-52$ K).[14] Above 1.8 K, no anomaly attributed to the occurrence of a magnetic ordering transition can be detected via magnetic susceptibility measurements. This result agrees with the specific heat measurements performed on CeRuSi, which reveal the absence of magnetic transition.[13] The $\chi_m^{-1}=f(T)$ curve for the hydride $CeRuSiH_{1.0}$, also follows, but above 50 K, a Curie-Weiss law with $\theta_p=-18$ K and $\mu_{eff}=2.59(3)\mu_B$/Ce mol. This last value agrees with that calculated for a free Ce^{3+} ion ($2.56\mu_B$). Below 50 K, the $\chi_m^{-1}=f(T)$ curve for hydride exhibits (i) a deviation from the Curie-Weiss law, which could be attributed to the crystal electric field effect and (ii) a minimum suggesting a magnetic transition. The increase of θ_p from −81 to −18 K in the sequence $CeRuSi \rightarrow CeRuSiH_{1.0}$ reveals that the hydrogenation induces a decrease of the Kondo interaction.

Figure 2 shows at low temperatures the temperature dependence of the magnetization divided by the applied magnetic field $M/\mu_0 H$ for $CeRuSiH_{1.0}$. For $0.1\ T \leqslant \mu_0 H \leqslant 0.5$ T [Fig. 2(a)], two maxima are clearly visible on the $M/\mu_0 H=f(T)$ curves. These measurements reveal the occurrence of two antiferromagnetic transitions for the hydride. The Néel temperatures, defined by the peaks observed in the $d(M/\mu_0 H)/dT=f(T)$ derivative curves, are $T_{N1}=7.5(2)$ K and $T_{N2}=3.1(2)$ K. Therefore, the hydrogenation of CeRuSi induces an interesting nonmagnetic $\rightarrow$ magnetic transition. Similar results were reported by H insertion in the intermediate valence indide CeNiIn (Ref. 26) and the Kondo insulator stannide CeNiSn.[27,28] In these cases, the hydrogenation also keeps the crystal symmetry of the initial intermetallic but induces an increase of the unit cell volume and the oc-

TABLE IV. Interatomic distances between Ce and its ligands in CeRuSi, $CeRuSiH_{1.0}$, and $CeRu_2Si_2$.

	CeRuSi[a]	$CeRuSiH_{1.0}$		$CeRu_2Si_2$[b]
Ce-4Ce	3.834	3.900		
Ce-4Ce	4.197	4.180	Ce-4Ce	4.195
Ce-4Ru	3.065	3.246	Ce-8 Ru	3.225
Ce-4Si	3.145	3.253	Ce-8Si	3.249
Ce-Si	3.426	3.609	Ce-2Si	3.573
Ce-Si	3.468	3.903		

[a]Reference 14.
[b]Reference 24.

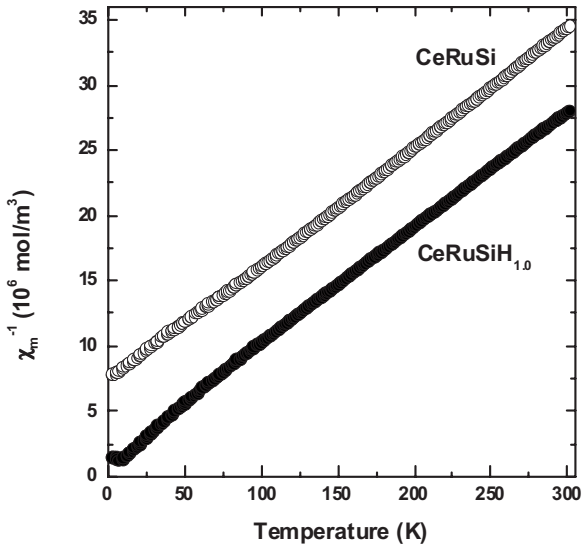

FIG. 1. Temperature dependence of the reciprocal magnetic susceptibility χ_m^{-1}, measured with an applied field $\mu_0 H=4$ T, of CeRuSi and its hydride.

currence of a ferromagnetic ($CeNiInH_{1.8}$) or antiferromagnetic ($CeNiSnH_{1.0}$) behaviors. These magnetic transitions can be explained by a decrease of the strength of the coupling J_{cf} between the $4f$(Ce) orbitals and conduction electrons, which governs the competition between Kondo and magnetic Ruderman-Kittel-Kasuya-Yoshida interactions within the well-known Doniach diagram. In this scheme, the hydrogenation can be considered as an application of "negative" pressure on intermetallic. Indeed, at this stage, it is also necessary to say that the H insertion into the intermetallics shifts the Fermi level, which is a consequence of the H-valence states. Recently, the modification of the electronic structures of CeNiIn and CeNiSn caused by the hydrogenation was investigated using a density-functional theory approach.[29,30] These calculations confirm a larger localization of the $4f$(Ce) states in the hydrides; the contribution at the Fermi level E_F from $4f$(Ce) states rises, for instance, from 2.4 to 8.7 eV^{-1} in the sequence $CeNiIn \rightarrow CeNiInH_{1.8}$.

The two antiferromagnetic transitions appearing, respectively, at T_{N1} and T_{N2} are differently influenced by the applied magnetic field. For instance, when $\mu_0 H$ increases from 0.75 to 2.0 T [Fig. 2(b)], (i) the maximum associated with the T_{N1} transition stays practically at the same temperature, but (ii) on the contrary, the maximum at T_{N2} is completely eliminated and the magnetization increases with decreasing temperature. This last result indicates the existence of a metamagnetic transition influencing the antiferromagnetic order defined by the T_{N2} temperature. At $\mu_0 H=1$ T, the two magnetic transitions appear at $T_{N1}=7.5(2)$ K (close to the maximum of the $M/\mu_0 H=f(T)$ curve) and $T_{T1}=4.7(2)$ K [temperature where the $d(M/\mu_0 H)/dT=f(T)$ derivative curve exhibits a negative maximum]. Finally, for 2.5 T $\leqslant \mu_0 H \leqslant 4$ T [Fig. 2(c)], the increase of M at low temperature is less pronounced and then disappears for $\mu_0 H=4$ T. The magnetization measurements versus temperature performed on a $CeRuSiH_{1.0}$ hydride suggests that it presents a complex magnetic phase diagram.

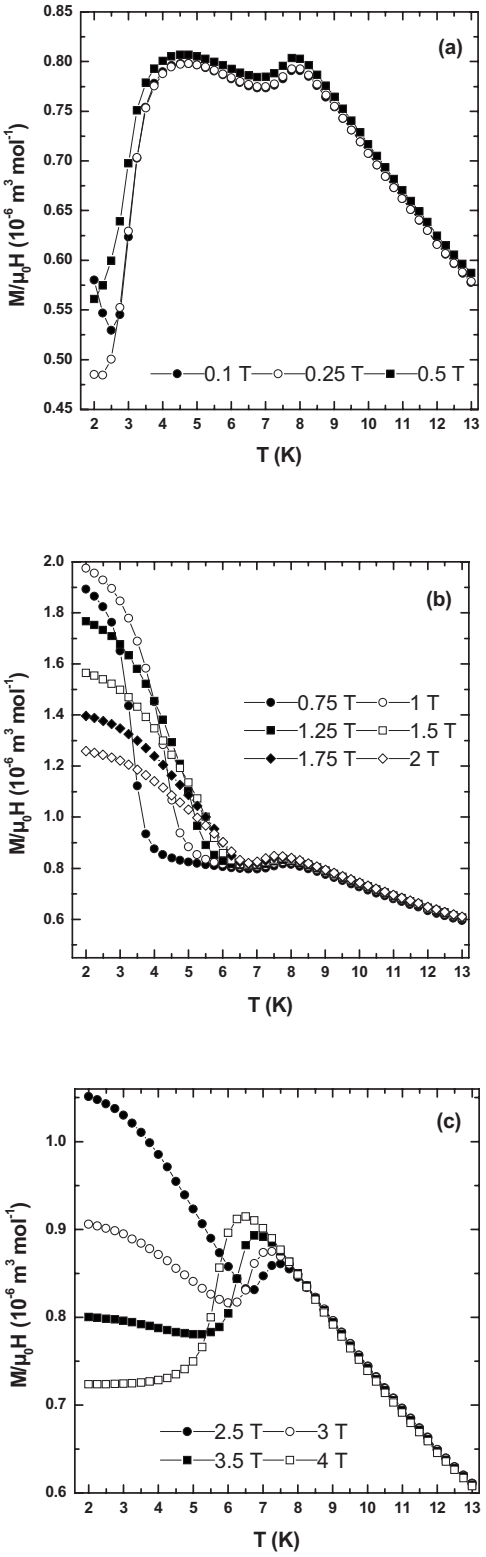

FIG. 2. Temperature dependence of the magnetization of hydride $CeRuSiH_{1.0}$ measured at various applied fields $\mu_0 H$.

The strong influence of the applied field on the magnetic properties of $CeRuSiH_{1.0}$ is illustrated in Fig. 3. Below the T_{N1} Néel temperature, the $M=f(\mu_0 H)$ curves, obtained at increasing field up to 4.6 T, are seen to exhibit two steplike

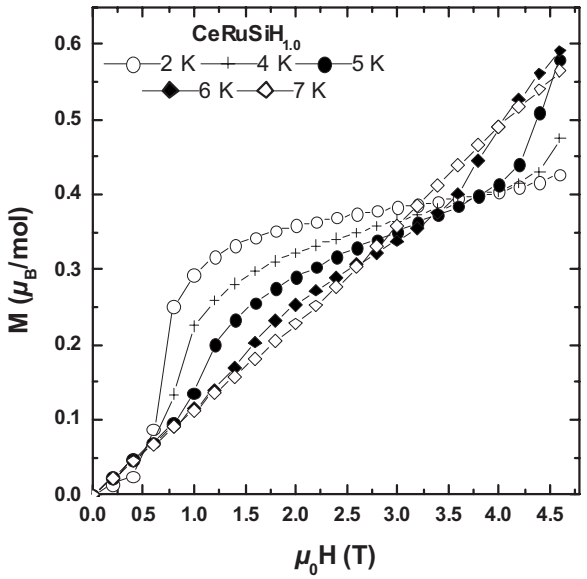

FIG. 3. Field dependence at various temperatures of the magnetization of $CeRuSiH_{1.0}$.

features at critical fields H_{C1} and H_{C2}. For instance, at 5 K, these fields are respectively equal to $H_{C1}=1.1(1)$ T and $H_{C2}=4.5(2)$ T. In the antiferromagnetic range ($T<T_{N1}$), the anomaly attributed to H_{C1} is always detected, whereas that appearing at H_{C2} is less pronounced with decreasing temperature. At 2 K, $H_{C1}=0.7(1)$ T can be determined, but it is not possible to obtain the value of H_{C2}.

Combining the results of this present study, we can draw a tentative magnetic phase diagram of $CeRuSiH_{1.0}$ (Fig. 4). Four magnetic phases are distinguished in the ordered state below $T_{N1}=7.5(2)$ K. Phases (I) and (II) correspond certainly to an antiferromagnetic arrangement. Phase (III), which appears between the two critical fields H_{C1} and H_{C2}, shows a ferrimagnetic character; at 2 K, the magnetization of the hydride for $H_{C1}<\mu_0 H<H_{C2}$ is about $0.4\mu_B$/Ce mol (Fig. 3). Finally, phase (IV) existing for $\mu_0 H>H_{C2}$ exhibits a higher magnetization (resulting eventually from a ferromagnetic order). More magnetization experiments performed at higher fields than 4.6 T are necessary in order to determine H_{C2} at low temperatures.

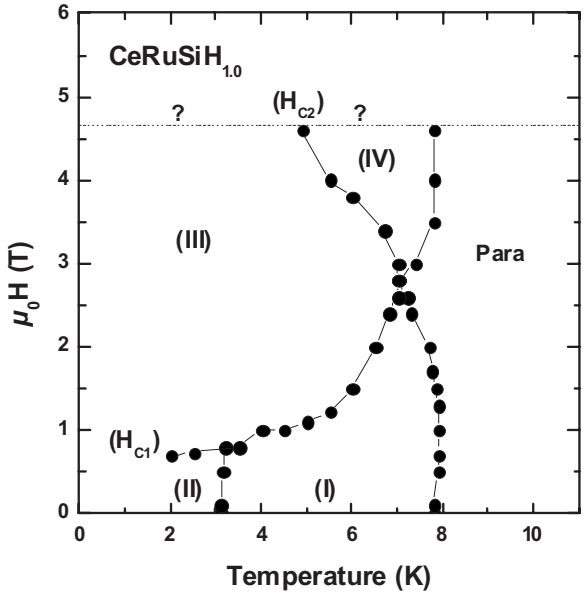

FIG. 4. Field-temperature phase diagram of hydride $CeRuSiH_{1.0}$ deduced from the magnetization measurements.

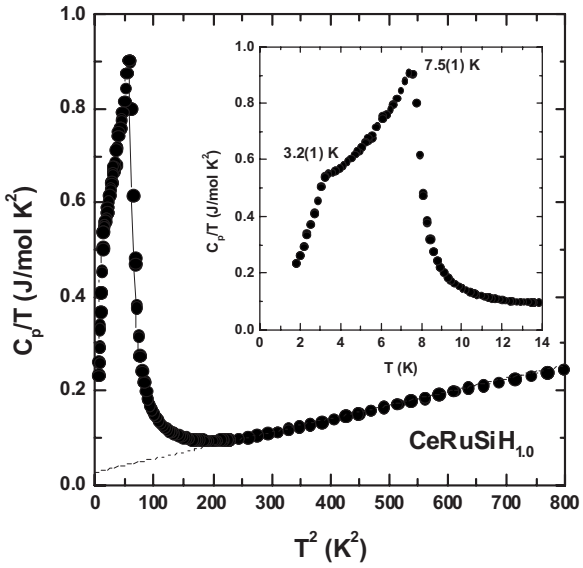

FIG. 5. C_p/T versus T^2 curve for $CeRuSiH_{1.0}$; the dashed line represents fit to the data in the paramagnetic range for 16 K$<T<$26 K (see text) (inset: C_p/T versus T curve).

The magnetic phase diagram of $CeRuSiH_{1.0}$ shows some similarities with those of $(Ce_{0.8}La_{0.2})Ru_2Si_2$ (Refs. 17, 20, and 31) and $CeRu_2(Si_{0.9}Ge_{0.1})_2$.[18,31,32] In these systems, a long-range magnetic order is induced in the heavy-fermion ternary silicide $CeRu_2Si_2$ by slightly expanding its lattice through the substitution of a few percent of lanthanum for cerium or germanium for silicon. These compounds exhibit two antiferromagnetic transitions [at 5.6(2) and 1.8(2) K for $(Ce_{0.8}La_{0.2})Ru_2Si_2$],[31] and these magnetic structures are strongly influenced by the applied magnetic field.

C. Specific heat

The specific heat (C_p) of $CeRuSiH_{1.0}$ has been measured at zero magnetic field between 1.8 and 50 K. As presented in Fig. 5 (inset), the temperature dependence of C_p divided by temperature exhibits a peak at about 7.5(1) K and a shoulder near 3.2(1) K. These temperatures agree with the Néel temperatures T_{N1} and T_{N2} reported above by magnetization measurements (Fig. 2) and confirm the antiferromagnetic behavior of $CeRuSiH_{1.0}$. Valuable information can be obtained from the entropy associated with the antiferromagnetic ordering, which is estimated from the magnetic contribution to the specific heat in the low-temperature range as $C_{p\ \mathrm{mag}}=C_p-(\gamma T+\beta T^3)$. Between 16 and 26 K, the fitting $C_p/T=\gamma+\beta T^2$ (Fig. 5) yields to an electronic coefficient $\gamma=26$ mJ/mol K^2 and phonon constant $\beta=2.86$

$\times 10^{-4}$ J/mol K^4). At T_{N1}, the magnetic entropy reaches $S_m = 3.473$ J/mol K or $0.60R \ln 2$, which is reduced from $R \ln 2 = 5.76$ J/mol K, the value expected for a doublet ground state of Ce^{3+}. This reduction suggests the presence of a rather weak Kondo effect in this hydride. This agrees with the small electronic term $\gamma = 26$ mJ/mol K^2 deduced from the fitting of the experimental data for $16\ \text{K} < T < 26\ \text{K}$ (Fig. 5). Considering the strong decrease of γ from 220 to 26 mJ/mol K^2 in the sequence CeRuSi $\rightarrow$ CeRuSiH$_{1.0}$, we can conclude that the hydrogenation affects the influence of the Kondo effect.

D. Electrical resistivity and thermoelectric power

The difference of behavior between CeRuSi and its hydride can also be evidenced on their transport properties. The electrical resistivities of these two compounds based on cerium and their equivalent nonmagnetic lanthanum compounds LaRuSi and LaRuSiH$_{1.0}$ have been measured experimentally in the temperature range 4.2–290 K, as shown in Figs. 6 and 7.

As observed previously,[13] the resistivity ρ of CeRuSi increases in a Kondo-like manner when the temperature decreases from 290 to about 45 K. At lower temperatures, ρ decreases rapidly with decreasing temperature. The ρ values measured here are smaller than that reported previously. For instance, for our CeRuSi sample, $\rho = 475\ \mu\Omega$ cm at the maximum around 45 K, whereas a value close to 1700 $\mu\Omega$ cm is reported in Ref. 13 at the same temperature. This difference could be associated with the anisotropic character of this ternary silicide.

Figure 6(a) shows the resistivities of CeRuSi and LaRuSi, as well as the difference $\rho_m = \rho(\text{CeRuSi}) - \rho(\text{LaRuSi})$. The ρ_m resistivity has a maximum at roughly 45 K and decreases above it, which is already a good indication for a crystalline field splitting of the order of 45 K and a Kondo behavior above it. We analyze the resistivity of CeRuSi and then of its hydride in the framework of the classical method[12] introduced to describe the Kondo contributions of cerium compounds such as $CeAl_2$ or $CeAl_3$. This method, which has been already very successful to derive the magnetic resistivity of many cerium compounds, assumes that the phonon contribution is taken equal to the total resistivity of an equivalent nonmagnetic compound and that the difference ρ_m gives, therefore, the magnetic resistivity. In our case, the application of this method and its validity are more questionable because the resistivities are quite large for metallic systems and our experimental values are different from those of Ref. 13. Moreover, as previously explained, this method can be considered as less necessary here than in other previous cases because the total resistivity of CeRuSi already decreases with temperature above its maximum. However, the plot shown in Fig. 6(b) improves clearly the description of both Kondo and crystalline field effects.

The log T variation of ρ_m, presented in Fig. 6(b), exhibits clearly a log T dependence between 80 and 290 K. This behavior is characteristic of the Kondo effect for the $4f^1$ configuration with a $(2j+1) = 6$ degeneracy and is observed for temperatures larger than the crystal field splitting Δ, which is

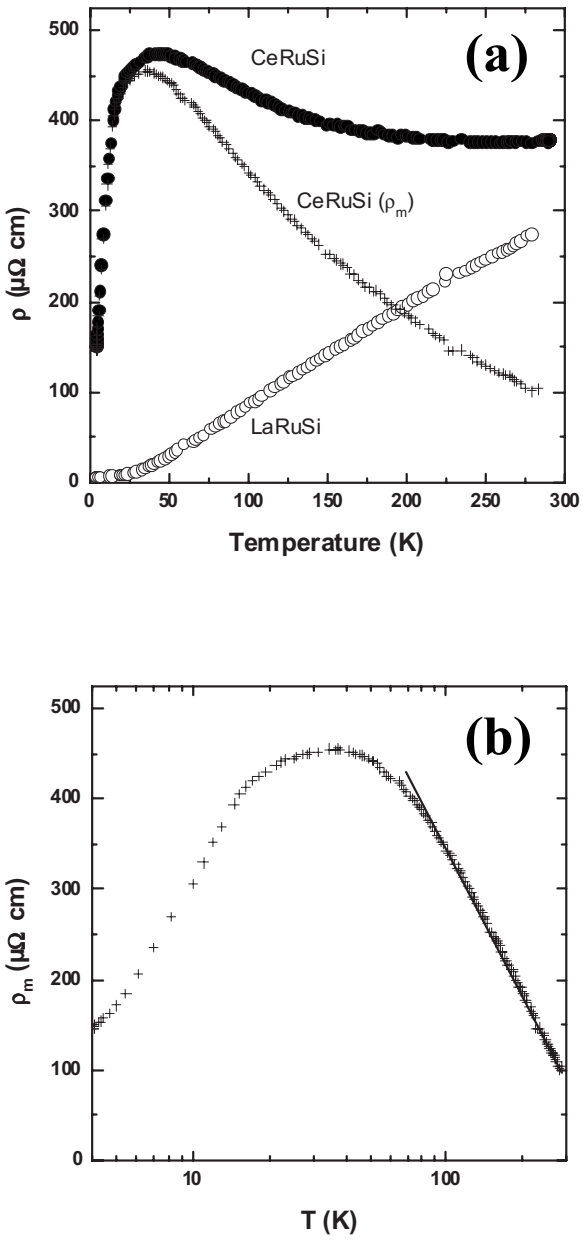

FIG. 6. (a) Temperature dependence of the electrical resistivity of CeRuSi and LaRuSi, and the difference (ρ_m) between these two ternary silicides. (b) ρ_m as a function of log T (solid line represents the fit: A log T).

given here by the maximum of ρ_m, i.e., $\Delta = 45$ K.[12] We obtain, from the log T slope of ρ_m, a large value of the exchange integral J for the s-f exchange Hamiltonian $H = J\mathbf{s_c} \cdot \mathbf{S_f}$, as in the case of other Kondo compounds. We have considered here only the explanation of the "high-temperature" regime above the Kondo temperature T_K. The rapid drop of the resistivity with decreasing temperature below Δ is certainly due to the low-temperature behavior below T_K, which can be estimated to be of the order of 10–20 K, according to resistivity and magnetic susceptibility measurements. A characteristic T^2 law of the low-temperature resistivity has been observed below 7 K by Rebelsky *et al.*[13] and is also visible here in Fig. 6(b). Finally, the effects of Kondo

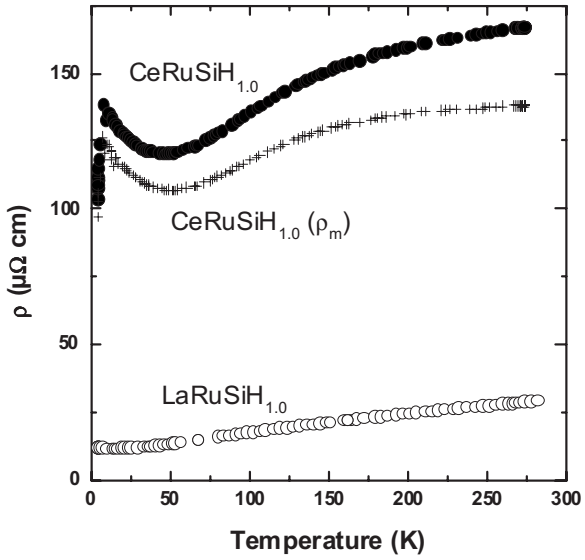

FIG. 7. Temperature dependence of the electrical resistivity of $CeRuSiH_{1.0}$ and $LaRuSiH_{1.0}$, and the difference (ρ_m) between these two hydrides.

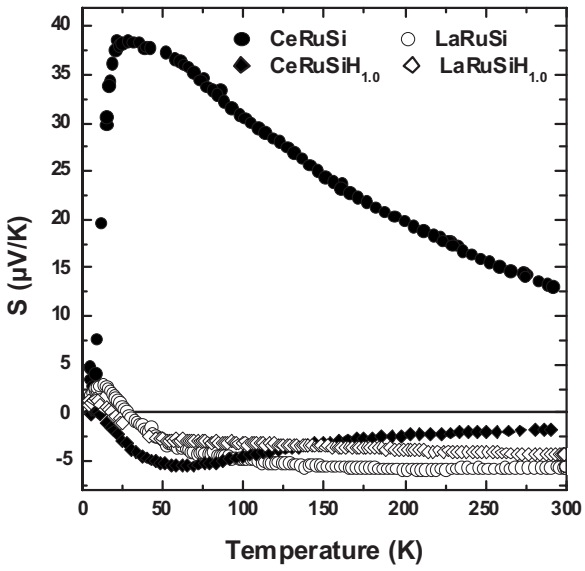

FIG. 8. Temperature dependence of the thermoelectric power for CeRuSi, LaRuSiH, and their hydrides.

and crystalline field at sufficiently high temperatures and the coherence effect at very low temperatures are separated from each other and are well observed in the resistivity of CeRuSi.

Figure 7 shows the resistivities of $CeRuSiH_{1.0}$ and $LaRuSiH_{1.0}$, as well as the difference $\rho_m = \rho(CeRuSiH_{1.0}) - \rho(LaRuSiH_{1.0})$. The magnetic resistivity ρ_m, as deduced by the method of Ref. 12, is here very close to the total resistivity because of the small value of the resistivity of the $LaRuSiH_{1.0}$ equivalent compound. Thus, we observe first a maximum near 7.8(2) K, which corresponds to the Néel temperature T_{N1} characteristic of an antiferromagnetic order, as already detected around 7.5(2) K by previously described magnetization measurements. Then, the resistivity decreases above T_{N1}, goes through a minimum at roughly 50 K, and then increases very slowly with a tendency to saturation above 150 K. However, up to 270 K, no maximum of ρ_m corresponding to the crystal field splitting in the Kondo model is observed.[12] We have to remark here that the resistivity of $LaRuSiH_{1.0}$ is very small and increases very smoothly and that it yields eventually a too small estimation of the phonon nonmagnetic part of the resistivity of $CeRuSiH_{1.0}$; taking a more rapidly increasing nonmagnetic part of the resistivity would have given a maximum of ρ_m corresponding to a crystal field splitting Δ typically of the order of 150–200 K.

Thus, the hydrogenation yields three effects here. First, one observes a change from a weak heavy-fermion Ce compound without any magnetic ordering and with a specific heat constant $\gamma = 220$ mJ/mol K^2 to a hydride having a small $\gamma = 26$ mJ/mol K^2 and presenting an antiferromagnetic order at roughly 7.5 K; clearly, hydrogenation shows *a priori* an opposite effect to pressure. Second, the crystal field splitting Δ increases very much from a value of 45 K to a value of the order of 150–200 K; this can be related to the structural changes, as indicated previously by the strong increase of the c/a ratio. Third, the value of the total resistivity decreases very much upon hydrogenation, and the hydride appears to be clearly more metallic. We will discus these effects later on.

The thermoelectric powers S of the four compounds CeRuSi, LaRuSi, and their hydrides have been measured, and the corresponding curves versus temperature from 4.2 to 290 K are plotted in Fig. 8. The thermoelectric power of CeRuSi is always positive, reaching a large value at its maximum of 25 K, while the thermoelectric power of the hydride $CeRuSiH_{1.0}$ remains small and negative with a minimum at roughly 65 K, except at very low temperatures where it presents a very small positive peak. The thermoelectric powers of the compounds LaRuSi and $LaRuSiH_{1.0}$ remain also negative and small, except also at very low temperatures where they are passing through small positive maxima. At first sight, we can say that only the thermoelectric power of CeRuSi is really large, while the three other thermoelectric powers are small and negative, as for normal metals. The analysis of the different contributions shows that the magnetic contribution is very close to the total thermoelectric power of these Ce compounds, so that we can analyze directly the behavior of the thermopowers of Ce compounds.

The theoretical calculation[33] of the thermoelectric power S of such compounds has been performed in a model describing the influence of the crystalline field effect on the Kondo effect at temperatures larger than the Kondo temperature T_K within the Coqblin-Schrieffer Hamiltonian for the $4f^1$ (or $4f^{13}$) configuration of cerium (or ytterbium). This calculation yields a maximum at a temperature equal to a fraction typically of the order of $\Delta/2 - \Delta/4$ of the total crystalline field splitting Δ. In this model, the shape of S depends on the values of the different involved parameters such as the exchange integral J and the direct scattering potential V. The first parameter, J, can be determined by the log T dependence of the magnetic resistivity, but the second parameter, V, is more difficult to be determined from experiment. However,

the peaks corresponding to the crystalline field effect are generally positive in Ce compounds and negative in Yb compounds. The thermoelectric power has also been computed with the same Hamiltonian at low temperatures below T_K, and a positive (or negative) peak has been obtained at a temperature roughly equal to $T_K/2$ for Ce (or Yb) compounds.[34]

More recently, the thermoelectric properties of intermetallic compounds with Ce ions were accounted for by the single-impurity Anderson model, which considers both the crystal field splitting Δ of the $4f$ ground state multiplet and a strong Coulomb repulsion.[35] The two important parameters are Δ and the coupling strength $\Gamma=\pi|V_{\mathrm{kf}}|^2 n_s(E_f)$ between the $4f$ electrons and the conduction electrons, where V_{kf} is the f-c hybridization parameter (or the mixing term of the Anderson Hamiltonian) and $n_s(E_f)$ the density of states for the conduction band at the Fermi energy; Γ is also the width of the hybridized f level. The parameter $|V_{\mathrm{kf}}|$ and consequently Γ are considered to increase with pressure, and this model has been applied successfully to account for the pressure dependence of both the electrical resistivity and the thermoelectric power of the $CeRu_2Ge_2$ compound.[36] Its thermoelectric power is negative and small at normal pressure, while, at small pressures, a very small positive peak appears at very low temperatures and another positive one at a temperature close to 300 K, and these two peaks are separated by a negative minimum at intermediate temperatures. When pressure increases again, the two positive peaks increase and the minimum in between becomes positive. At very high pressures above 10 GPa, the thermoelectric power is always positive, becomes very large of the order of 60 μV/K and still has a maximum at a temperature of the order of 200–250 K. Such a behavior has been theoretically accounted for within the single-impurity Anderson model of Ref. 35 by taking a constant crystal field splitting $\Delta=0.07$ eV and a Γ value increasing with pressure from 0.06 eV for the normal pressure to 0.15 eV for the high pressure of 10 GPa.[36]

Let us try now to explain the present experimental data. The thermoelectric power S of CeRuSi has a maximum at a temperature roughly equal to half the value Δ of the crystal field splitting deduced from the resistivity measurements. In fact, the thermoelectric power of CeRuSi looks like that of $CeAl_3$, which is, however, a much stronger heavy-fermion compound. Thus, the thermoelectric power of CeRuSi can be well accounted for by the previous calculation for $T>T_K$.[33] On the other hand, the thermoelectric powers of the three compounds $CeRuSiH_{1.0}$, LaRuSi, and $LaRuSiH_{1.0}$ are negative and very small, of the order of $\cong 5$ μV/K. In order to be more quantitative, the thermoelectric powers of the nonmagnetic compounds LaRuSi and $LaRuSiH_{1.0}$ are negative, very small, and not varying very much with temperature except at very low temperatures: these curves can be considered as the "normal" state without any hybridization. On the other hand, the thermoelectric power of $CeRuSiH_{1.0}$, although still very small and mostly negative, has a very small positive peak corresponding to the ordering temperature and another broad peak at roughly 60 K. Indeed, we can propose that this negative peak is due to the crystalline field effect,[33] and then we obtain a value of Δ typically of the order of 150–300 K, which is in rough agreement with our previous conclusions from the analysis of the electrical resistivity data. Finally, the thermoelectric power of CeRuSi is characteristic of a moderate heavy-fermion one with a crystal field effect well described by the previous model of Ref. 33 developed for $T<T_K$. Then, we can account for the change of the thermopower from CeRuSi to $CeRuSiH_{1.0}$ by taking an important decrease of the hybridization coupling Γ with hydrogenation, exactly opposite to the effect of pressure used to describe the case of the $CeRu_2Ge_2$ compound.[36]

Let us now analyze the change of behavior from CeRuSi to $CeRuSiH_{1.0}$. CeRuSi is a moderate heavy-fermion compound that does not order magnetically and has an electronic specific heat constant $\gamma=220$ mJ/mol K^2, while $CeRuSiH_{1.0}$ is an antiferromagnet that presents a smaller γ coefficient (26 mJ/mol K^2). We can interpret this change by the use of the Doniach diagram.[37] This well-known theoretical diagram gives the variation of the Néel temperature T_N versus the product $|Jn_s(E_f)|$ of the exchange integral J by the density of states $n_s(E_f)$ of the conduction band at the Fermi energy: T_N increases first, then passes through a maximum, and tends to zero at the quantum critical point Q for a critical value of $|Jn_s(E_f)|$. The Doniach diagram separates magnetically ordered (generally with an antiferromagnetic order) compounds (such as $CeAl_2$) that have relatively small γ values, for small values of $|Jn_s(E_f)|$ below point Q, from typical heavy-fermion compounds (such as $CeAl_3$) that do not order magnetically and have large γ values, for large values of $|Jn_s(E_f)|$ above point Q. It is well known that the pressure increases the value of J (Ref. 38) and one goes from the first category of compounds to the second one under high pressure. Pressure decreases the atomic volume of the considered system, while here hydrogenation increases the atomic volume and has the effect opposite to pressure. Thus, it results that hydrogenation decreases the value of $|Jn_s(E_f)|$, and its effect on the Doniach diagram can perfectly explain the important change of behavior from CeRuSi to its hydride. The decrease of γ by a factor of order 10 can be fairly accounted for by a huge change of the parameter J, which is approximately similar to the change when passing from the compound $CeAl_3$ to $CeAl_2$.

IV. CONCLUSION

The hydrogenation of the Ce compounds crystallizing in the tetragonal CeFeSi-type induces two antagonist effects: An anisotropic expansion of the unit cell and the occurrence of Ce-H bonding. The competition between these two effects can lead to the demagnetization of the cerium, as observed for hydride $CeCoSiH_{1.0}$,[2,4,5] or, on the contrary, to the appearance of a magnetic order, as reported here for $CeRuSiH_{1.0}$. This competition seems to be steered by the value of the interatomic distance $d_{\mathrm{Ce\text{-}H}}=2.447$ Å between the cerium and the hydrogen. This distance is the highest in the hydride $CeRuSiH_{1.0}$. Recent analyses of the electronic structures and of the chemical bonding properties of this hydride using the covalent bond energy suggest that the bonding effect of hydrogen does not prevail here over cell expansion, which favors the magnetic ordering.[39] After hydrogenation, a

larger localization of the $4f$(Ce) states is evidenced by non-spin-polarized calculations. H insertion drives CeRuSi from a Kondo regime to a magnetic order with a weak Kondo effect.

$CeRuSiH_{1.0}$ exhibits a complex magnetic phase diagram where two antiferromagnetic transitions have been observed. Furthermore, a metamagnetic double transition was evidenced at low temperature. This diagram shows many similarities with that reported for a $CeRu_2(Si_{1-x}Ge_x)_2$ system,[31,32,40,41] where a long-range antiferromagnetic order is induced in the heavy-fermion $CeRu_2Si_2$ by slightly expanding its lattice through the substitution of a few percent of germanium instead of silicon. A similar effect has been observed in $Ce_{1-x}La_xRu_2Si_2$ alloys, where the change from Ce to La expands the lattice and favors the magnetic ordering.[17] Now, the investigation of hydride $CeRuSiH_{1.0}$ by neutron powder diffraction is in progress in order to explain its magnetic phase diagram.

ACKNOWLEDGMENTS

The authors would like to thank R. Decourt for his assistance during the electrical resistivity and thermoelectric power measurements. Finally, B. Chevalier, J. Rodriguez Fernandez, and B. Coqblin thank the European Science Foundation (ECOM-COST action P16) for financial support.

*Corresponding author; chevalie@icmcb-bordeaux.cnrs.fr

[1] G. Wiesinger and G. Hilscher, *Handbook of Magnetic Materials*, edited by K. H. J. Buschow (Elsevier Science, New York, 1991), Vol. 6, p. 511.
[2] V. Paul-Boncour, J. Alloys Compd. **367**, 185 (2004).
[3] W. Xiang-Zhong, K. Donnely, J. M. D. Coey, B. Chevalier, J. Etourneau, and T. Berlureau, J. Mater. Sci. **23**, 329 (1988).
[4] S. Wirth, R. Skomski, and J. M. D. Coey, Phys. Rev. B **55**, 5700 (1997).
[5] K. Miliyanchuk, L. Havela, A. V. Kolomiets, and A. V. Andreev, J. Alloys Compd. **404-406**, 165 (2005).
[6] B. Chevalier, E. Gaudin, F. Weill, and J.-L. Bobet, Intermetallics **12**, 437 (2004).
[7] B. Chevalier and S. F. Matar, Phys. Rev. B **70**, 174408 (2004).
[8] B. Chevalier, M. Pasturel, J.-L. Bobet, and O. Isnard, Solid State Commun. **134**, 529 (2005).
[9] B. Chevalier, S. F. Matar, J. Sanchez Marcos, and J. Rodriguez Fernandez, Physica B **378-380**, 795 (2006).
[10] B. Chevalier, S. F. Matar, M. Ménetrier, J. Sanchez Marcos, and J. Rodriguez Fernandez, J. Phys.: Condens. Matter **18**, 6045 (2006).
[11] B. Chevalier, J. S. Marcos, J. R. Fernandez, M. Pasturel, and F. Weill, Phys. Rev. B **71**, 214437 (2005).
[12] B. Cornut and B. Coqblin, Phys. Rev. B **5**, 4541 (1972).
[13] L. Rebelsky, K. Reilly, S. Horn, H. Borges, J. D. Thompson, J. O. Willis, R. Aikin, R. Caspari, and C. D. Bredl, J. Appl. Phys. **63**, 3405 (1988).
[14] R. Welter, G. Venturini, B. Malaman, and E. Ressouche, J. Alloys Compd. **202**, 165 (1993).
[15] O. Isnard, S. Miraglia, R. Welter, and B. Malaman, J. Synchrotron Radiat. **6**, 701 (1999).
[16] J. D. Thompson, J. O. Willis, C. Godart, D. E. MacLaughlin, and L. C. Gupta, Solid State Commun. **56**, 169 (1985).
[17] M. J. Besnus, J. P. Kappler, P. Lehmann, and A. Mayer, Solid State Commun. **55**, 779 (1985).
[18] C. Godart, A. M. Umarji, L. C. Gupta, and R. Vijayaraghavan, Phys. Rev. B **34**, 7733 (1986).
[19] P. Haen, J. Flouquet, F. Lapierre, P. Lejay, and G. Remenyi, J. Low Temp. Phys. **67**, 391 (1987).
[20] S. Quezel, P. Burlet, J. L. Jacoud, L. P. Régnault, J. Rossat-Mignod, C. Vettier, P. Lejay, and J. Flouquet, J. Magn. Magn. Mater. **76-77**, 403 (1988).
[21] J.-L. Bobet, S. Pechev, B. Chevalier, and B. Darriet, J. Alloys Compd. **267**, 136 (1998).
[22] V. Petricek and M. Dusek, *The crystallographic computing system Jana 2000* (Institute of Physics, Praha, Czech Republic, 2000).
[23] P. Dordor, E. Marquestaut, and G. Villeneuve, Rev. Phys. Appl. **15**, 1607 (1980).
[24] C. Godart, C. Ammarguellat, M. F. Ravet, N. Wetta, C. Levy-Clement, H. Noel, and G. Krill, Solid State Commun. **59**, 241 (1986).
[25] L. P. Regnault, W. A. C. Erkelens, J. Rossat-Mignod, P. Lejay, and J. Flouquet, Phys. Rev. B **38**, 4481 (1988).
[26] B. Chevalier, M. L. Kahn, J.-L. Bobet, M. Pasturel, and J. Etourneau, J. Phys.: Condens. Matter **14**, L365 (2002).
[27] B. Chevalier, M. Pasturel, J.-L. Bobet, J. Etourneau, O. Isnard, J. Sanchez Marcos, and J. Rodriguez Fernandez, J. Magn. Magn. Mater. **272-276**, 576 (2004).
[28] V. A. Yartys, B. Ouladdiaf, O. Isnard, O. Yu. Khyzhun, and K. H. J. Buschow, J. Alloys Compd. **359**, 62 (2003).
[29] S. F. Matar, B. Chevalier, V. Eyert, and J. Etourneau, Solid State Sci. **5**, 1385 (2003).
[30] A. Aburto and E. Orgaz, Phys. Rev. B **75**, 045130 (2007).
[31] J.-M. Mignod, L.-P. Regnault, J.-L. Jacoud, J. Rossat-Mignod, P. Haen, and P. Lejay, Physica B **171**, 357 (1991).
[32] J.-M. Mignod, Ph. Boutrouille, L.-P. Regnault, P. Haen, and P. Lejay, Solid State Commun. **77**, 317 (1991).
[33] A. K. Bhattacharjee and B. Coqblin, Phys. Rev. B **13**, 3441 (1976).
[34] V. Zlatic, B. Horvatic, I. Milat, B. Coqblin, G. Czycholl, and C. Grenzebach, Phys. Rev. B **68**, 104432 (2003).
[35] V. Zlatic and R. Monnier, Phys. Rev. B **71**, 165109 (2005).
[36] H. Wilhelm, D. Jaccard, V. Zlatic, R. Monnier, B. Delley, and B. Coqblin, J. Phys.: Condens. Matter **17**, S823 (2005).
[37] S. Doniach, *Proceedings of the International Conference on Valence Instabilities and Related Narrow-Band Phenomena*, edited by R. D. Parks (Plenum, New York, 1976), p. 168.
[38] B. Coqblin, *Tenth Training Course in the Physics of Correlated Electron Systems and High Tc Superconductors, Salerno, Italy, October 2005*, edited by A. Avella and F. Mancini (AIP Conference Proceedings Vol. 846, 2006), p. 3.
[39] S. F. Matar, Phys. Rev. B **75**, 104422 (2007).
[40] S. Süllow, G. J. McIntyre, P. Haen, B. D. Rainford, and T. Fukuhara, J. Magn. Magn. Mater. **226-230**, 179 (2001).
[41] P. Haen, H. Bioud, and T. Fukuhara, Physica B **259-261**, 85 (1999).